Z-scaled *K*-shell dielectronic recombination rate coefficients

Arati Dasgupta[1] and K. G. Whitney[2]
[1]*Radiation Hydrodynamics Branch, Plasma Physics Division, Naval Research Laboratory, Washington, D.C. 20375, USA*
[2]*Berkeley Scholars Incorporation, Springfield, Virginia 22150, USA*
(Received 24 September 2003; published 3 February 2004)

State-specific dielectronic recombination (DR) rate coefficients from ground states of H- and He-like Al, Ti, Ni, Kr, and Mo ions have been calculated in the isolated resonance and intermediate coupling approximation. The data generated for these calculations consists of energies of singly and doubly excited states, radiative rates, autoionization rates, and dielectronic recombination branching ratios. A Hartree-Fock method that includes relativistic corrections was employed in order to carry out the calculations. Three parameter fits to the data were then made using the Al, Ti, and Kr data to obtain scaling relations that enable one to calculate similar data for other ions by interpolation in the range between Al and Kr and somewhat beyond by extrapolation. The scaling accuracy was verified by comparing the scaling relation predictions to detailed data obtained for Ni and Mo calculations. The results obtained also compared well with other published work in which total ground state to ground state dielectronic recombination rates were calculated. The DR rate coefficients that are calculated from the scaled DR data are generally most accurate for intermediate to high-temperature collisional plasmas. However, in low-temperature photoionized plasmas, significant DR contributions come from the $\Delta n=0$ core excitations that are not present for *K*-shell recombination and thus one should expect the *Z* scaled DR rates to be accurate for any range of temperatures of interest.

DOI: 10.1103/PhysRevA.69.022702 PACS number(s): 34.80.Kw

I. INTRODUCTION

It is well known that dielectronic recombination (DR), the inverse of the Auger process, is an important recombination process for plasmas with moderate to high atomic number, *Z*, ions [1,2]. These processes have a significant effect on the ionization balance of plasmas in the temperature range of maximum equilibrium abundance. Reliable DR data are crucial for inferring plasma conditions from line identifications in emission spectra and for making accurate x-ray laser gain calculations and plasma diagnostics for laboratory and astrophysical plasmas. The dielectronic satellite lines appearing on the long-wavelength side of resonance lines are often used for diagnosing electron temperature. Several different theoretical methods starting from simple semiempirical formulas to very complex calculations have been performed to calculate this important DR data [3–5].

There exist a number of published DR rate coefficients in the isoelectronic sequence of H-like [6–11] and especially He-like [12–14] ions. Most of these works that employ detailed calculations present results for only a few ions in the isoelectronic sequence, while others that apply more broadly use approximate methods [15–17] or involve rapid evaluation of DR rates using fitting formulas [18]. Although these formulas are sometimes obtained from accurately calculated data, one can estimate from them only a total ground-to-ground DR rate which is inadequate since state-specific rates are often needed. Since *ab initio* DR calculations involve a large number of doubly and singly excited levels of the recombined ions, the bookkeeping becomes overwhelming and computations are very time consuming, and repeating the same calculations for each ion in an isoelectronic sequence unnecessarily tasks human and computational resources and is prone to errors.

There has been recent interest in calculating reliable low-temperature DR rates to support the analysis of data obtained from launches of the new high-resolution x-ray satellite Chandra and XMM-Newton. These investigations concentrate on obtaining very accurate DR rates for low-density photoionized plasmas. Most authors, therefore, expend huge amounts of time and resources to obtain these low-temperature DR rates by using complex close-coupling methods such as the *R*-matrix method. It was, however, pointed out by Gorczyca *et al.* [19] that simpler perturbative methods sometimes predict better results than *R*-matrix calculations in the determination of DR rate coefficients. Thus, one can predict reasonably accurate DR rate coefficients for a wide range of electron temperature using perturbative methods for applications that involve moderate density laboratory as well low-density collisionally ionized astrophysical plasmas. We have employed such methods to explicitly calculate the DR data for Al, Ti, Ni, Kr, and Mo ions in the H- and He-like isoelectronic sequences and we provide all the state-specific scaling data that is needed to predict the same for other ions of interest in these same sequences with reasonable accuracy. More specifically, we therefore present all the scaling coefficients needed to obtain state-specific DR rates from excited states energies and DR branching ratios of ions in the *K* shell, of Al through Mo. In order to obtain a total DR rate, one needs only to use this data summed over all of the intermediate and the singly excited levels of the recombined ion.

We first calculate the DR rate coefficients and other related data of H-like and He-like Al, Ti, and Kr ions by using the Hartree-Fock with relativistic corrections method of Cowan [20]. We then determine three-parameter polynomial fits to this data which consists of energies, autoionization rates, radiative rates, and the DR branching ratios. These

scaling relations can then be used to obtain the *K*-shell DR data for any ion between Al and Kr and also somewhat beyond without repeating these elaborate computations for other ions. To check and verify the validity of scaling for an ion within this range as well as beyond Kr, we performed detailed calculations for *K*-shell Ni and Mo ions. The efficacy of *Z* scaling was first reported in a previous calculation by Dasgupta and Whitney [21] in which we presented DR data for the F-like isoelectronic sequence. We also reported DR data for O-like ions [22] and demonstrated the scalability of these data by computing detailed DR data for Mo^{+34} [23] and comparing it to the same data obtained from the scaling relations. However in the above mentioned papers four-parameter fits to the data were made in contrast to the three-parameter fits that are found to be sufficient for this present work.

A very brief description of the theoretical method is given in Sec. II, and in Sec. III, we present the results of our calculations and make comparisons with other published works. Section IV contains a brief summary of the various approximations involved in and the estimated validity of this work.

II. THEORY AND CALCULATIONS

Here, we briefly describe the theoretical aspects of DR and review only the most important considerations and formulas that are needed to calculate the DR data. A more detailed description of our calculational method can be found in Ref. [21].

The Maxwellian averaged DR rate coefficient α^{DR}, at a temperature T, which takes an ion from an initial state $|i\rangle$ into a final recombined state $|k\rangle$ through all intermediate autoionizing states $|j\rangle$ is given by

$$\alpha^{DR}(i,k)=\left[\frac{4\pi\mathcal{R}}{kT}\right]^{3/2}\frac{a_0^3}{2g_i}\sum_j F_{ijk}\exp(-\varepsilon_j/kT), \quad (1)$$

where the DR branching ratio F_{ijk} is given by

$$F_{ijk}\equiv\frac{g_j A^A_{ji}A^R_{jk}}{\sum_{i'}A^A_{ji'}+\sum_{k'}A^R_{jk'}}. \quad (2)$$

In this formula, ε_j is the energy of the doubly excited state measured with respect to the initial state, g_i and g_j are the statistical weights of the initial ion state $|i\rangle$ and doubly excited state $|j\rangle$, respectively, a_0 is the Bohr radius and $\mathcal{R}$ is the Rydberg energy. In Eq. (2) the denominator sums go over all possible autoionization states $|i'\rangle$ (including autoionizations to excited states) and and all possible final recombined states $|k'\rangle$. A^A_{ji} and A^R_{jk} are the autoionization and radiative rates from the doubly excited autoionization state $|j\rangle$ to initial state $|i\rangle$ and final state $|k\rangle$, respectively. The autoionization rates are calculated from the perturbation expression,

$$A^A_{ji}=(2\pi/\hbar)|\langle(\gamma_i J_i),l_i,J_t|H|\gamma_j J_j\rangle|^2, \quad (3)$$

TABLE I. Configuration labeling of singly excited He-like states.

c	Configuration	c	Configuration
1	$1s2s$	7	$1s4p$
2	$1s2p$	8	$1s4d$
3	$1s3s$	9	$1s4f$
4	$1s3p$	10	$1s5l$
5	$1s3d$	11	$1snl(6\leqslant n\leqslant 20)$
6	$1s4s$		

and the radiative electric dipole transition probability from state j to a lower state k is given in terms of a reduced dipole matrix element by

$$A^R_{jk}=\left[\frac{4\omega^3_{jk}}{3\hbar c^3(2J_j+1)}\right]|\langle\gamma_k J_k|D|\gamma_j J_j\rangle|^2, \quad (4)$$

where γ_j is used to designate all quantum numbers other than J_j, the total angular momentum. $\gamma_i J_i$, $\gamma_j J_j$, and $\gamma_k J_k$ define the initial target state, the resonance capture state, and the final recombined state. The free electron has orbital angular momentum l_i and D is the electric dipole operator for the electromagnetic interaction.

In order to calculate the DR rate from an initial level i to a final level k, one has to calculate many F_{ijk}s and then sum over all resonance states j. By working at the fine-structure level, one creates an enormous amount of data. In order to specialize to atomic models that are detailed yet compact enough to require only moderate amounts of data, we have chosen to work at the configuration level. As mentioned in Refs. [21,22], DR data at the configuration level produce sufficient and accurate results for most detailed ionization calculations of noncoronal plasmas.

At the configuration level, a notational change is made, and i, j, and k go over into a, b, c in all the previous equations. In the present work, we include intermediate resonance states $2lnl'$ and $1s2lnl'$ for recombination from the initial ground state, $1s$ or $1s^2$, for H- and He-like ions, respectively. The radiative rates and autoionization rates were calculated explicitly for $n\leqslant 20$ and $l\leqslant 6$ for H-like ions and $n\leqslant 15$ and $l\leqslant 6$ for He-like ions. For higher Rydberg states, we employed the usual $1/n^3$ extrapolation procedure for the autoionization rates. The doubly and singly excited levels and all the rates associated with them were judiciously lumped to develop our configuration averaged model. In Tables I and II we list the configurations of the recombined singly excited states, denoted as c, which are contained in our calculations, while Tables III and IV contain the doubly excited configurations, b, for the He- and Li-like ions along with the scaling coefficients for their energies [see Eq. (7)]. For DR from H-like ions at the configuration level (Table III), our model consists of 31 He-like unlumped intermediate configuration states and two lumped states consisting of $2snl$ and $2pnl$ states with $7<n\leqslant 20$ and $0<l\leqslant 6$. Similarly for He- to Li-like recombination, as listed in Table IV, the doubly excited states consist of 31 $1s2lnl'$ configurations with

TABLE II. Configuration labeling of singly excited Li-like states.

c	Configuration	c	Configuration
1	$1s^2 2s$	7	$1s^2 4p$
2	$1s^2 2p$	8	$1s^2 4d$
3	$1s^2 3s$	9	$1s^2 4f$
4	$1s^2 3p$	10	$1s2s5l$
5	$1s^2 3d$	11	$1s2snl(6\leqslant n\leqslant 15)$
6	$1s^2 4s$		

$l=0$ and 1 and with $2\leqslant n\leqslant 7$, $0\leqslant l'\leqslant 6$ and two lumped states consisting of $1s2snl$ and $1s2pnl$ states with $7<n<20$ and $l\leqslant 6$. All energies, radiative rates, and autoionization rates were calculated in the intermediate coupling and multiconfiguration Hartree-Fock approximation using the

TABLE III. Energy scaling coefficients for the doubly excited-state levels of He-like configurations. $X[Y]$ means $X\times 10^Y$.

b	Configuration	b_0^{**}	b_1^{**}	b_2^{**}
1	$2s2p$	5.253[−1]	−0.422	5.150
2	$2p^2$	5.332[−1]	−0.597	6.817
3	$2s3p$	6.679[−1]	−0.646	5.950
4	$2p3s$	6.737[−1]	−0.820	7.206
5	$2p3p$	6.759[−1]	−0.872	7.655
6	$2p3d$	6.778[−1]	−0.904	8.048
7	$2s4p$	7.179[−1]	−0.759	6.310
8	$2p4s$	7.251[−1]	−0.967	7.839
9	$2p4p$	7.260[−1]	−0.987	8.014
10	$2p4d$	7.268[−1]	−1.002	8.176
11	$2p4f$	7.271[−1]	−1.004	8.217
12	$2s5p$	7.411[−1]	−0.814	6.480
13	$2p5s$	7.486[−1]	−1.033	8.081
14	$2p5p$	7.491[−1]	−1.043	8.183
15	$2p5d$	7.495[−1]	−1.049	8.238
16	$2p5f$	7.496[−1]	−1.051	8.270
17	$2p5g$	7.497[−1]	−1.053	8.295
18	$2s6p$	7.536[−1]	−0.845	6.567
19	$2p6s$	7.614[−1]	−1.067	8.203
20	$2p6p$	7.616[−1]	−1.072	8.244
21	$2p6d$	7.619[−1]	−1.077	8.293
22	$2p6f$	7.620[−1]	−1.081	8.337
23	$2p6g$	7.621[−1]	−1.081	8.336
24	$2p6h$	7.620[−1]	−1.080	8.332
25	$2s7p$	7.611[−1]	−0.858	6.559
26	$2p7s$	7.690[−1]	−1.088	8.274
27	$2p7p$	7.691[−1]	−1.087	8.254
28	$2p7d$	7.693[−1]	−1.092	8.303
29	$2p7f$	7.694[−1]	−1.094	8.327
30	$2p7g$	7.693[−1]	−1.092	8.303
31	$2p7h$	7.694[−1]	−1.096	8.353
32	$2p7i$	7.695[−1]	−1.097	8.365
33	$2snl(8\leqslant n\leqslant 20)$	7.790[−1]	−0.897	6.621
34	$2pnl(8\leqslant n\leqslant 20)$	7.830[−1]	−1.124	8.363

TABLE IV. Energy scaling coefficients fo the doubly excited levels of Li-like configurations. $X[Y]$ means $X\times 10^Y$.

b	Configuration	b_0^{**}	b_1^{**}	b_2^{**}
1	$1s2s2p$	5.246[−1]	−0.793	4.802
2	$1s2p^2$	5.324[−1]	−0.891	6.283
3	$1s2s3p$	6.671[−1]	−1.271	5.763
4	$1s2p3s$	6.726[−1]	−1.386	6.928
5	$1s2p3p$	6.748[−1]	−1.417	7.325
6	$1s2p3d$	6.766[−1]	−1.439	7.646
7	$1s2s4p$	7.169[−1]	−1.469	6.160
8	$1s2p4s$	7.239[−1]	−1.608	7.585
9	$1s2p4p$	7.248[−1]	−1.624	7.782
10	$1s2p4d$	7.255[−1]	−1.631	7.894
11	$1s2p4f$	7.259[−1]	−1.638	7.976
12	$1s2s5p$	7.401[−1]	−1.568	6.378
13	$1s2p5s$	7.474[−1]	−1.712	7.867
14	$1s2p5p$	7.479[−1]	−1.719	7.956
15	$1s2p5d$	7.483[−1]	−1.725	8.040
16	$1s2p5f$	7.484[−1]	−1.728	8.073
17	$1s2p5g$	7.485[−1]	−1.726	8.047
18	$1s2s6p$	7.526[−1]	−1.619	6.459
19	$1s2p6s$	7.601[−1]	−1.768	8.011
20	$1s2p6p$	7.604[−1]	−1.773	8.069
21	$1s2p6d$	7.606[−1]	−1.776	8.114
22	$1s2p6f$	7.607[−1]	−1.777	8.126
23	$1s2p6g$	7.607[−1]	−1.777	8.134
24	$1s2p6h$	7.607[−1]	−1.776	8.121
25	$1s2s7p$	7.601[−1]	−1.651	6.527
26	$1s2p7s$	7.677[−1]	−1.801	8.083
27	$1s2p7p$	7.678[−1]	−1.800	8.080
28	$1s2p7d$	7.680[−1]	−1.805	8.143
29	$1s2p7f$	7.681[−1]	−1.808	8.167
30	$1s2p7g$	7.682[−1]	−1.809	8.179
31	$1s2p7h$	7.681[−1]	−1.807	8.154
32	$1s2p7i$	7.681[−1]	−1.807	8.154
33	$1s2snl(8\leqslant n\leqslant 15)$	0.776	−1.717	6.623
34	$1s2pnl(8\leqslant n\leqslant 15)$	0.780	−1.855	8.218

computer codes of R. D. Cowan. We have taken into account Coster-Kronig transitions, $1s2pnl\rightarrow 1s2s+e^-$, from autoionizing Rydberg states in calculating the radiative branching ratios for recombinations from He-like ions. The atomic data we calculated includes all autoionization and radiative rates explicitly for $n\leqslant 20$ for H-like and $n\leqslant 15$ for He-like recombination. A $1/n^3$ extrapolation procedure for the branching ratios was then employed to calculate the contributions from higher Rydberg states. We have neglected radiative cascades to autoionizing states since this generally reduces the DR rate coefficients, but only by a few percent [12].

Z scaling of DR data

The relations for scaling energies of singly (ε_c) and doubly (ε_b) excited states, total autoionization ($\Sigma_{a'}A^A_{ba'}$), total

radiative ($\Sigma_{c'}A^R_{bc'}$) rates, and DR branching ratios F_{abc} with atomic number for ions in the fluorine and oxygen isoelectronic sequence were presented and discussed in Refs. [21,22]. In the configuration averaged model the DR branching ratio F_{abc} is given by

$$F_{abc}=\frac{g_b A^A_{ba} A^R_{bc}}{\sum_{a'} A^A_{ba'}+\sum_{c'} A^R_{bc'}}, \tag{5}$$

where a' and c' refer to all possible initial and final recombined configurations, respectively. The DR rate coefficients then can be calculated for any ion between Al and Mo using

$$\alpha^{DR}(a,c)=\left[\frac{4\pi\mathcal{R}}{kT}\right]^{3/2}\frac{a_0^3}{2g_a}\sum_b F_{abc}\exp(-\varepsilon_b/kT). \tag{6}$$

To calculate DR rate coefficients, one needs scaling relations for ε_b and F_{abc}. The configuration averaged energy ε_b scales as

$$\varepsilon_b=Z^2(b_0^{**}+b_1^{**}/Z+b_2^{**}/Z^2)_b, \tag{7}$$

where Eq. (7) is in units of eV. The coefficients in these equations were determined by requiring that they reproduce the DR data that was calculated for Al, Ti, and Kr.

One can obtain an indirect Z scaling of F_{abc} from the scaling relations of the configuration averaged A^A_{ba}, A^R_{bc}, $\Sigma_{a'}A^A_{ba'}$, and $\Sigma_{c'}A^R_{bc'}$ using Eq. (5). However a configuration averaged scaling for branching ratio F_{abc} can also be calculated directly from explicitly calculated F_{ijk}, in which case the scaling relation is given by the three-coefficients polynomial,

$$F_{abc}=Z^2(b_0^F+b_1^F/Z+b_2^F/Z^2) \tag{8}$$

(in units of s^{-1}).

III. RESULTS

We present state specific and also total DR data for H-like and He-like ions in this section. Configuration averaged DR rates to specific excited states c of the recombined ion are calculated from Eq. (6) for Al, Ti, and Kr using detailed calculations of the average energies of the doubly excited states ϵ_b and the branching ratios F_{abc}. These data are then used to obtain the scaling coefficients of Eqs. (7) and (8). From the scaling relations of these quantities one can then obtain the rate coefficients for any moderate atomic number ion in the H and He isoelectronic sequence. Total DR rates are then obtained by summing the state-specific rates over all the singly excited levels c. The DR rates obtained this way will include only the channels that are used in the configuration averaging scheme of our atomic model. This scheme includes the most dominant channels that constitute more than 96% of the total DR rates that are calculated from unaveraged and extrapolated data.

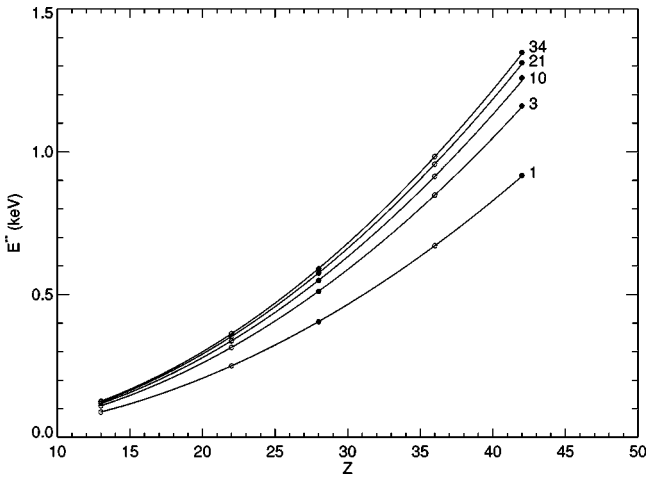

FIG. 1. Variation of energies of the five He-like doubly excited states, which are listed in Table III, as a function of Z. The curves are three-parameter fits to the three calculated points shown as *open circles* for Al^{11+}, Ti^{20+}, and Kr^{34+} and the *solid circles* are the calculated data for Ni^{26+} and Mo^{40+}.

A. Z scaling of DR data

Tables III and IV list the three-parameter scaling coefficients b_0^{**}, b_1^{**}, and b_2^{**}, given in Eq. (7), for each of the doubly excited states. These coefficients were determined from the configuration averaged data obtained from explicitly calculated doubly excited-state energies for Al, Ti, and Kr ions. The doubly excited-state energies of other ions in the sequence can now be obtained more simply from Eq. (7) rather than by repeating the detailed first-principles calculation. Figures 1 and 2 display the three-parameter polynomial fits to the doubly excited-state energies that we obtained for five of these levels in He- and Li-like ions, respectively. They contain the data points for He-like and Li-like Al, Ti, and Kr ions from which the curves were calculated. As a validity check of the scaling, we also present the explicitly

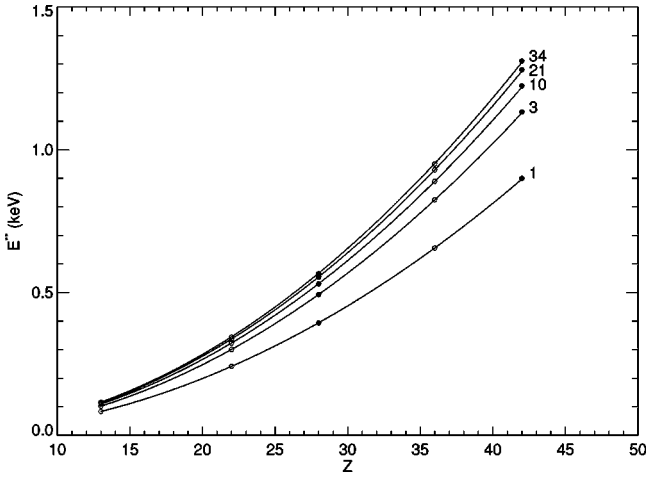

FIG. 2. Variation of energies of the five Li-like doubly excited states, which are listed in Table IV, as a function of Z. The curves are three-parameter fits to the three calculated points shown as *open circles* for Al^{10+}, Ti^{19+}, and Kr^{33+} and the *solid circles* are the calculated data for Ni^{25+} and Mo^{39+}.

calculated He-like and Li-like Ni and Mo doubly excited-states energies for these levels in the figures. As can be seen from Figs. 1 and 2, the data points for Ni and Mo ions fall right on the curves.

Since the energies of the doubly excited-states scale very smoothly, the scaling of the DR rates depends on how well the branching ratios F_{abc} scale with Z. Scaling coefficients of the configuration averaged DR branching ratios F_{abc} can be determined by obtaining the scaling relations for the configuration-averaged autoionization rates A^A_{ba} and radiative rates A^R_{bc} and then using them in Eq. (5). These rates are obtained by configuration averaging the directly calculated state specific A^A_{ji} and A^R_{jk}. The scaling relations for these quantities are not presented here, however, since there is another simpler way to scale the F_{abc}s by directly averaging the detailed F_{ijk} given in Eq. (2). These two approaches generally produce somewhat different scaling behavior [21]; however, because of their weak dependence on Z, we chose to scale the branching ratios from the directly averaged F_{abc} values of Al, Ti, and Kr by adopting the three coefficient polynomial fit given by Eq. (5). These coefficients are given in Tables V and VI for H-like and He-like recombination processes, respectively. As mentioned before, the 33 dominant DR channels given in each of these two tables constitute more than 96% of the contribution to the total DR rates. Figures 3 and 4, which contain these three-parameter polynomial curves for a few of the He- and Li-like DR channels for recombination of H- and He-like ions, show that the branching ratios do not depend strongly on Z. Also shown in these figures are the calculated data points of the three ions Al, Ti, and Kr, from which the fitting was obtained. To check on and confirm the smoothness of the scaling of these ratios, we calculated the same ratios for Ni ions (with Z falling within) and for Mo ions (with Z beyond the range of the Al-Kr ions) and present them also in Figs. 3 and 4. The actual data points that are used for scaling are shown as open circles and the Ni and Mo data points are shown as closed circles which fall on or very close to the curves in all cases but one. The calculated $F_{1,1,1}$ for Mo^{39+}, shown in Fig. 4, is much higher than that predicted by scaling and $F_{1,8,6}$ for this same ion is somewhat lower. However, as will be demonstrated in the following section, this does not have any noticeable effect on the total rates, and the total scaled DR rates for Mo ions are in excellent agreement with our calculated rates.

TABLE V. Scaling coefficients for the He-like DR branching ratios F_{abc}. Here $a=1$ is the ground $1s$. $X[Y]$ means $X\times10^{Y}$.

b	c	b_0^F	b_1^F	b_2^F
1	1	−4.439[11]	4.123[13]	−3.451[14]
2	2	−2.091[12]	1.638[14]	−1.587[15]
3	1	−1.566[11]	1.325[13]	−1.143[14]
4	3	−2.327[11]	1.440[13]	−9.206[13]
5	2	−2.840[11]	1.960[13]	−1.828[14]
5	4	−1.180[12]	8.015[13]	−7.345[14]
6	5	−3.281[11]	2.025[13]	−7.196[13]
7	1	−6.729[10]	5.621[12]	−4.873[13]
8	6	−6.019[10]	3.584[12]	−3.813[12]
9	2	−6.297[10]	3.914[12]	−3.102[13]
9	7	−6.190[11]	3.818[13]	−2.911[14]
10	8	−1.317[11]	7.979[12]	3.675[12]
11	9	−6.018[9]	3.784[11]	4.645[12]
12	1	−3.444[10]	2.871[12]	−2.497[13]
13	10	−1.799[10]	1.042[12]	8.644[12]
14	2	−1.308[10]	7.980[11]	−4.393[12]
14	10	−2.447[11]	1.483[13]	−6.991[13]
15	10	−5.065[10]	3.058[12]	2.144[13]
16	10	−4.905[9]	3.031[11]	3.599[12]
17	10	−1.989[8]	1.252[10]	7.318[10]
18	1	−1.992[10]	1.658[12]	−1.443[13]
19	11	−6.844[9]	3.855[11]	7.811[12]
20	2	−3.258[9]	1.977[11]	−4.434[11]
20	11	−1.003[11]	6.042[12]	−2.267[12]
21	11	−2.370[10]	1.431[12]	1.860[13]
22	11	−3.294[9]	2.042[11]	2.567[12]
23	11	−2.034[8]	1.274[10]	8.374[10]
24	11	−4.090[6]	2.534[8]	5.644[8]
25	1	−1.287[10]	1.054[12]	−9.184[12]
26	11	−2.760[9]	1.545[11]	6.006[12]
27	2	−1.006[9]	6.061[10]	8.277[10]
27	11	−4.617[10]	2.756[12]	1.408[13]
28	11	−1.235[10]	7.468[11]	1.437[13]
29	11	−2.098[9]	1.314[11]	1.913[12]
30	11	−1.710[8]	1.073[10]	6.846[10]
31	11	−5.897[6]	3.620[8]	4.561[8]
32	11	−7.002[4]	4.000[6]	−3.939[6]
33	1	−3.687[10]	2.770[12]	−2.417[13]
34	2	−6.779[8]	4.092[10]	3.248[11]
34	11	−9.934[10]	5.899[12]	1.576[14]

B. Total DR rate coefficients

We present the total DR rate coefficients, α^{DR}(total), for H- and He-like Al, Ti, and Kr ions here, where $\alpha^{DR}(total) = \Sigma_{a,c}\alpha^{DR}(a,c)$ and $\alpha^{DR}(a,c)$ is calculated from Eqs. (6)–(8) for any ion in the range $13 \leqslant Z \leqslant 42$. We also present the total DR rate coefficients obtained for Ni and Mo in order to check on the validity of the scaling, since, while the DR rates for Ni and Mo were explicitly calculated as was done for Al, Ti, and Kr, they were not used to calculate the scaling coefficients. Although we generated state specific DR data for Ni and Mo, we do not present this data here, since the configuration averaged state-specific rates for these ions are more easily obtained from Eq. (6) using the scaling coefficients. The scaled DR rates thus obtained do not include extrapolated contributions from very high Rydberg levels and thus are smaller but within 5% of those calculated explicitly from the detailed levels.

A number of total DR rates for H- and He-like ions are shown in Figs. 5 and 6. Figure 5 contains the DR rate coefficients for recombination from H-like to He-like ions. The solid curves show our total DR rates for Al^{12+}, Ti^{21+}, Ni^{27+}, Kr^{35+}, and Mo^{41+}, which were calculated using the detailed levels and then extrapolated for high Rydberg levels of the

TABLE VI. Scaling coefficients for the Li-like DR branching ratios F_{abc}. Here $a=1$ is the ground $1s^2$. $X[Y]$ means $X\times 10^Y$.

b	c	b_0^F	b_1^F	b_2^F
1	1	−1.608[11]	1.702[13]	−1.482[14]
2	2	−9.734[11]	1.118[14]	−1.135[15]
3	1	−1.184[11]	1.182[13]	−1.061[14]
4	3	−7.641[10]	1.278[12]	−2.785[13]
5	2	−2.651[11]	2.334[13]	−2.049[14]
5	4	−7.741[11]	5.184[13]	−3.448[14]
6	5	−2.281[11]	1.655[13]	−6.513[13]
7	1	−4.030[10]	4.444[12]	−4.011[13]
8	6	−1.830[9]	1.735[12]	−2.136[13]
9	2	−2.143[11]	1.447[13]	−1.271[14]
9	7	−8.800[10]	9.467[12]	−2.534[13]
10	8	−7.831[10]	6.041[12]	5.633[12]
11	9	−4.975[9]	4.311[11]	1.149[12]
12	1	−1.890[10]	2.169[12]	−1.963[13]
13	10	−1.227[10]	1.287[12]	−1.401[13]
14	2	−8.621[10]	6.094[12]	−5.129[13]
14	10	−5.211[10]	5.027[12]	−1.260[13]
15	10	−3.061[10]	2.628[12]	1.120[13]
16	10	−3.631[9]	3.265[11]	1.034[12]
17	10	−1.568[8]	1.317[10]	−1.562[10]
18	1	−1.047[10]	1.223[12]	−1.109[13]
19	11	−9.454[9]	7.990[11]	−8.285[12]
20	2	−3.624[10]	2.918[12]	−2.418[13]
20	11	−4.302[10]	3.401[12]	−1.073[13]
21	11	−1.385[10]	1.317[12]	9.685[12]
22	11	−2.458[9]	2.210[11]	8.069[11]
23	11	−1.615[8]	1.368[10]	−1.361[10]
24	11	−3.129[6]	2.523[8]	−8.701[8]
25	1	−6.480[9]	7.619[11]	−6.907[12]
26	11	−6.401[9]	4.966[11]	−4.961[12]
27	2	−1.893[10]	1.651[12]	−1.359[13]
27	11	−3.137[10]	2.310[12]	−7.801[12]
28	11	−7.111[9]	7.459[11]	7.317[12]
29	11	−1.740[9]	1.549[11]	5.414[11]
30	11	−1.339[8]	1.133[10]	−1.000[10]
31	11	−3.771[6]	3.192[8]	−1.039[9]
32	11	−5.660[4]	4.217[6]	−2.916[7]
33	1	−1.413[10]	1.721[12]	−1.564[13]
34	2	−4.132[10]	3.735[12]	−3.364[13]
34	11	−1.244[11]	9.250[12]	−1.608[13]

captured electron. The total configuration averaged DR rate coefficients obtained using the scaling relations are also shown as solid circles in this graph for H-like Fe^{25+}, Ni^{27+}, and Mo^{41+}. For Ni^{27+}, the calculated and scaled results are mostly identical, whereas for Mo, there is almost exact agreement for low-temperature rates and the differences for higher temperatures are less than 2%. The lower values are attributed mainly to the fact that the scaled results were obtained from a lesser number of DR channels in our averaging scheme. We also show a comparison of our results for H-like DR rate coefficients with those of Karim and Bhalla [7] in this figure. We see that for Fe, our scaled results are slightly lower than those of Ref. [7]. The very small difference could again be due to the fact that these scaled rates are obtained from averaged and not the detailed levels. For Ti^{21+}, the results of Ref. [7] are very slightly lower than our explicitly calculated DR rates.

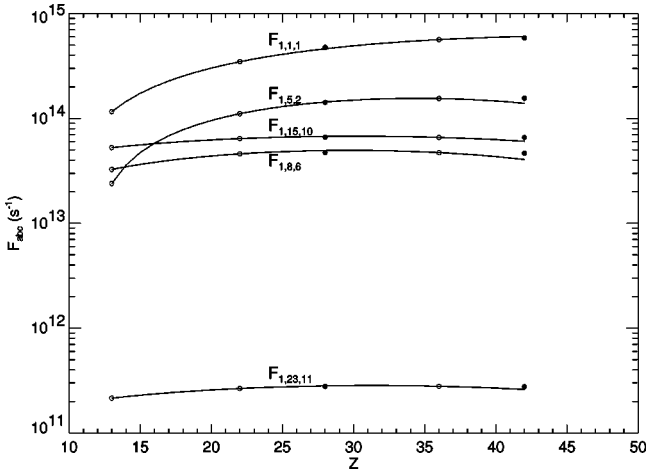

FIG. 3. Three-parameter polynomial curves for F_a obtained with the coefficients listed in Table V for recombination from H-like ions. The *open circles* are calculated data points and the *solid circles* are scaled branching ratios.

In Fig. 6 we present total DR rates for recombination from He-like ions for the same ions as in Fig. 5. As explained in the previous paragraph, total DR rate coefficients were again obtained by calculating the detailed branching ratios from all the doubly and singly excited states in our model and then by extrapolating for excited levels of the captured electron with very high Rydberg states. All the scaled data were again obtained from smaller configuration averaged sets of levels. We see very similar trends in our detailed vs scaled data as in the case for H-like recombination. For Ni^{26+}, these two rates are almost exactly identical

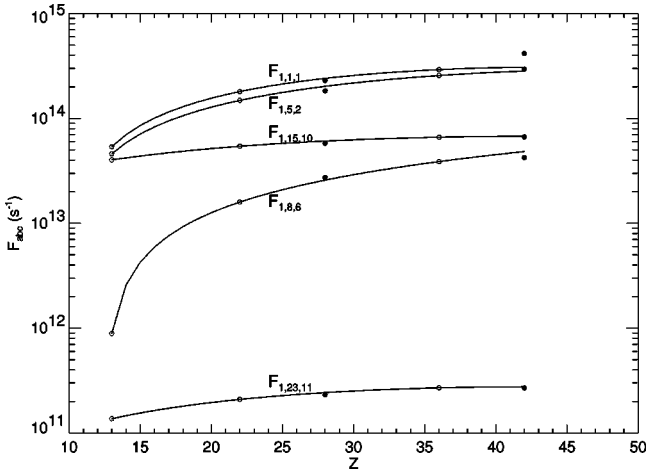

FIG. 4. Three-parameter polynomial curves for F_{abc} obtained with the coefficients listed in Table VI for recombination from He-like ions. The *open circles* are calculated data points and the *solid circles* are scaled branching ratios.

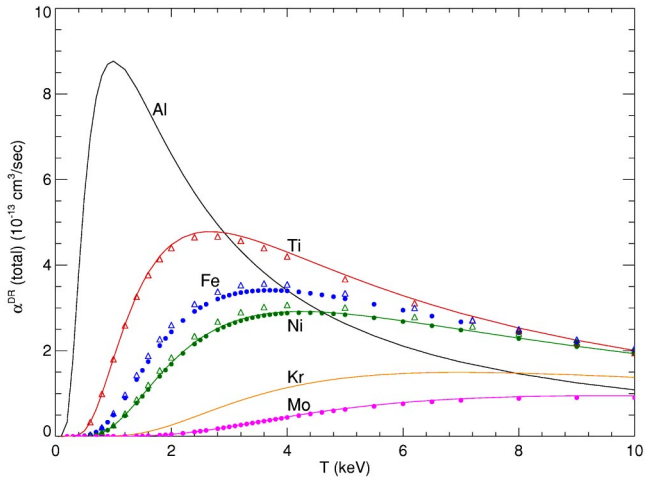

FIG. 5. Total dielectronic recombination rate coefficients for recombination from the ground state of H-like ions. Also shown are the scaled rate coefficients for Fe^{25+}, Ni^{27+}, and Mo^{41+} (*solid circles*) for comparison with calculations and other predictions. The *open triangles* are the results of Karim *et al.* [14,8].

whereas for ions with increasing Z such as for Mo^{40+}, there is complete agreement between the two rates at low temperatures, while, for higher temperatures the scaled data are somewhat smaller by a very small amount. This is expected since at low temperatures most of the recombination proceeds through the low-lying autoionizing levels which are included properly in the scaling relations. In this figure, we also compare our results with the multiconfiguration Dirac-Fock calculation of Chen [12] and the Hartree-Fock-Slater calculation of Karim and Bhalla [14]. The excellent agreement of our calculated results with the more complex multiconfiguration relativistic results of Chen for Mo is very encouraging. We also have very good agreement with Chen

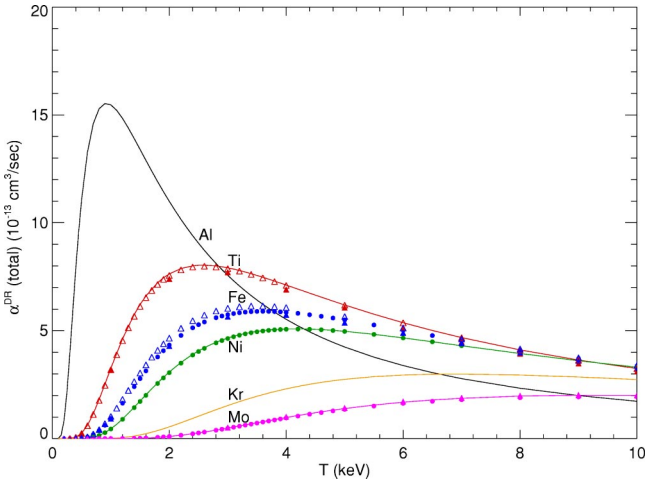

FIG. 6. Total dielectronic recombination rate coefficients for recombination from the ground state of He-like ions. Also shown are the scaled rate coefficients for Fe^{24+}, Ni^{26+}, and Mo^{40+} (*solid circles*) for comparison with calculations and other predictions. The *solid* and *open triangles* are the results of Chen [12] and Karim *et al.* [14], respectively.

with our calculated results for Ti^{20+} and scaled results for Fe^{24+}. At very high temperatures, our results for both Ti^{20+} and Fe^{24+} are slightly higher than those of Chen. When we compare our rates to those of Ref. [14], we notice very good agreement for Ti^{20+} but their DR rates for Fe^{24+} are slightly higher than our scaled rates.

IV. SUMMARY

In modeling the K- or L-shell ionization dynamics of moderate-Z elements, one is often concerned about two important and sometimes conflicting issues: the need for reliable atomic data and the need to acquire a large and adequate amount of atomic data. A good test of the reliability of small sets of scalable data created from detailed calculations is to compare them with other published results. Once there is satisfactory agreement between the scaleable data with other accurate results, the necessity of handling a large amount of data in ionization calculation by way of scaling relations is not only practical but sometimes crucial. In this paper, we have presented the scaling relations for calculations of DR data for H-like and He-like ions that not only will reduce future work for any such ions in the third and fourth rows of the periodic table, but by lumping fine-structure levels and thereby reducing the number of states, it will lessen the bookkeeping and make it easier to manage, the (still large amount of) atomic data.

We have demonstrated that our detailed DR rates are in excellent agreement with other sophisticated calculations and that the rates produced using the scaling coefficients generated from configuration-averaged state calculations give very comparable and therefore reasonably accurate DR rate coefficients. All the important DR channels necessary for the correct descriptions of charge state distributions were included in the calculations. Our results compare very well with the calculations of Chen [12] and Karim *et al.* [7,8,14]. Chen used a fully relativistic method as opposed to the semirelativistic method used by us and by Karim *et al.* However as mentioned by Chen [12,6], the effect of relativity is to reduce the total DR rate by only a few percent for moderate Z ions. We have also neglected any radiative cascades, i.e., radiative decays to autoionization states that are above the ionization limit. Chen [12] estimated this cascade effect and found that it reduced the total DR coefficients by less than 3%. Configuration interactions among the resonance states, were also neglected in our calculation, as this effect is expected to be small for H- and He-like ionization stages [24]. This neglect is not generally valid, however, in DR calculations involving more than a few electrons (see Ref. [25]). In general we found that DR data such as the energies of doubly and singly excited states, autoionization and radiative rates and DR branching ratios scale very smoothly with atomic number for both H- and He-like ions. Our experience with the scaling of recombination from F-like and O-like ions [21–23] was somewhat different. Although the energies varied very smoothly from one element to another, the scaling for the branching ratios were not always smooth. In the K

shell, however, these branching ratios scaled very smoothly, and we expect smooth scaling of DR data for the higher ionization stages in the *L* shell as well, such as for Li- and Be-like ions. But that has yet to be determined.

ACKNOWLEDGMENTS

This work was supported by DTRA and the Office of Naval Research.

[1] H.P. Summers, Mon. Not. R. Astron. Soc. **169**, 663 (1974).
[2] B.L. Whitten, A.U. Hazi, M.H. Chen, and P.L. Hagelstein, Phys. Rev. A **33**, 2171 (1986).
[3] A. Burgess, Astrophys. J. **141**, 1589 (1965).
[4] A.L. Merts, R.D. Cowan, and N.H. Magee, Jr., Los Alamos Scientific Laboratory Report No. LA-6220-**MS**, 1976 (unpublished).
[5] T.W. Gorczyca, F. Robicheaux, M.S. Pindzola, and N.R. Badnell, Phys. Rev. A **54**, 2107 (1996).
[6] M.H. Chen, Phys. Rev. A **38**, 3280 (1988).
[7] K.R. Karim and C.P. Bhalla, Phys. Rev. A **37**, 2599 (1988); C.P. Bhalla and K.R. Karim, *ibid.* **34**, 3525 (1986); K.R. Karim and C.P. Bhalla, *ibid.* **34**, 4743 (1986).
[8] K.R. Karim, M. Ruesink, and C.P. Bhalla, Phys. Rev. A **46**, 3904 (1992).
[9] L.A. Vainshtein and U.L. Safronova, At. Data Nucl. Data Tables **21**, 49 (1978).
[10] J. Nilsen, At. Data Nucl. Data Tables **37**, 191 (1987).
[11] K.B. Fournier, M. Cohen, and W.H. Goldstein, Phys. Rev. A **56**, 4715 (1997).
[12] M.H. Chen, Phys. Rev. A **33**, 994 (1986).
[13] M.H. Chen, Phys. Rev. A **38**, 6430 (1988).
[14] K.R. Karim and C.P. Bhalla, Phys. Rev. A **39**, 3548 (1989).
[15] S.M. Younger, J. Quant. Spectrosc. Radiat. Transf. **A29**, 67 (1983).
[16] J. Nilsen, J. Phys. B **19**, 2401 (1986).
[17] I. Nasser and Y. Hahn, J. Quant. Spectrosc. Radiat. Transf. **A29**, 1 (1983).
[18] H. Teng and Z. Xu, J. Quant. Spectrosc. Radiat. Transf. **A56**, 443 (1996).
[19] T.W. Gorczyca and N.R. Badnell, and D.W. Savin, Phys. Rev. A **65**, 062707 (2002).
[20] R.D. Cowan, *The Theory of Atomic Structure and Spectra* (University of California Press, Berkeley, 1981), p. 062707-1.
[21] A.D. Dasgupta and K.G. Whitney, Phys. Rev. A **42**, 2640 (1990).
[22] A.D. Dasgupta and K.G. Whitney, At. Data Nucl. Data Tables **58**, 77 (1994).
[23] A.D. Dasgupta and K.G. Whitney, J. Phys. B **28**, 515 (1995).
[24] R.D. Cowan and D.C. Griffin, Phys. Rev. A **36**, 26 (1987).
[25] T.W. Gorczyca and N.R. Badnell, Phys. Rev. A **54**, 4113 (1996).